Structural Studies of MJ1529, an O^6-methylguanine-DNA Methyltransferase

Anne Roberts, Jeffrey G. Pelton and David E. Wemmer[†]
Department of Chemistry, University of California and Physical Biosciences Division, Lawrence Berkeley National Lab, Berkeley, CA 94720-1460

[†]corresponding author:
David Wemmer
Dept. of Chemistry, MC-1460
University of California
Berkeley, CA 94720-1460 USA

dewemmer@LBL.gov
telephone: 510 486 4318
fax: 510 486 6059

This work was supported by the Office of Biological and Environmental Research, Office of Science of the Department of Energy under contract DE-AC03-76SF00098 to the Lawrence Berkeley National Laboratory. Funding for equipment was provided by the National Science Foundation (DMB 8609035 and BBS 8720134).

short title:
Structure of an O^6-MeG DNA Methyltransferase

keywords: NMR, protein structure, DNA Methyltransferase, DNA repair

Structural Studies of MJ1529, an O^6-methylguanine-DNA Methyltransferase

Anne Roberts, Jeffrey G. Pelton and David E. Wemmer
Department of Chemistry, University of California and Physical Biosciences Division, Lawrence Berkeley National Lab, Berkeley, CA 94720-1460

ABSTRACT

The structure of an O^6-methylguanine methyltransferase from the thermophile *Methanococcus jannaschii* has been determined using multinuclear multidimensional NMR spectroscopy. The structure is similar to homologues from other organisms that have been determined by crystallography, with some variation in the N-terminal domain. The C-terminal domain is more highly conserved in both sequence and structure. Regions of the protein show broadening reflecting conformational flexibility that is likely related to function.

INTRODUCTION

The survival and propagation of an organism are dependent on the integrity and faithful replication of its DNA. Modifications or alterations to DNA can be caused by external sources (UV radiation or chemical agents), endogenous metabolites, and naturally occurring errors in incorporation of nucleotides during DNA replication. Each may result in deleterious effects on the cell. To avoid such effects, a number of DNA repair systems have evolved to prevent these potentially harmful modifications from being propagated during DNA replication: Base-Excision Repair (BER); Nucleotide Excision Repair (NER); and Direct Reversal (DR) repair. These DNA repair systems are highly conserved among all branches of life. While the first two systems involve multiple enzymes to cleave, excise, and replace the damaged DNA, DR involves single enzymes which can repair the damaged base without removing nucleotides [1-3].

A prominent protein that functions in direct reversal is O^6-MethylGuanine-DNA MethylTransferase (MGMT) or AlkyGuanine alkylTransferase (AGT.) Alkylating agents such

as *N*-methyl-*N'*-nitro-*N*-nitrosoguanidine (MNNG) and *N*-methyl-*N*-nitrosourea (MNU) covalently modify DNA by alkylating the N^7 and O^6 position of guanine, and the O^4 position of thymine. Although N^7 alkylated guanine is the predominant alkylation product, this modification is relatively harmless as it does not affect the natural base pairing. In contrast, O^6-methylguanine (O^6MG), a much less common product, is a mutagenic, carcinogenic, and potentially cytotoxic lesion [4,5]. Incorporation of the methyl group leads to a preference for pairing of the modified guanosine with thymine rather than its normal Watson-Crick partner cytosine. This greatly increases the chance of incorporation of thymine opposite O^6MG during subsequent replication, resulting in a GC→ AT mutation (Figure 1)[6].

MGMT repairs O^6MG and to a lesser extent, O^4 methylthymine, by covalently transferring the methyl (or alkyl) group to the protein. A cysteine residue in the protein acts as a nucleophile and displaces the methyl group on the guanine, restoring the original base. Once the protein is methylated there is no mechanism to dealkylate the protein, thus, MGMT is known as a "suicide" repair protein; one protein molecule is used to repair one alkyl lesion [7]. Although MGMT protects against alkylation induced carcinogenesis, much interest in MGMT stems from the fact that alkylating and chloroethylating agents are used as chemotherapeutic treatments for their cytotoxicity. Although the mechanism for alkylation induced cell death is not completely understood (it appears to involve the MisMatch Repair-MMR system) alkylating agents do precipitate early cell death, and are used in the treatment of some forms of cancer [8,9]. By repairing O^6MG and other products formed by these agents, MGMT interferes with the cell-killing effects of treatments. Thus, effective inhibitors of MGMT are of great interest; one in particular, O^6-benzylguanine (O^6BG) has been used in clinical trials [9].

Investigation of the kinetics of repair by MGMT reveals that in both human MGMT

(hMGMT) and *E. coli* AdaC (the C-terminal domain of the Ada protein which has MGMT activity), repair of a single O^6MG lesion within single or double-stranded DNA is extremely fast, 10^5-10^8 $M^{-1}s^{-1}$, approaching the diffusion limited rate [10-12]. The repair process is facilitated by the physical interaction of the protein and DNA. In a study by *Pegg et al*. the authors showed that incubation of the free O^6MG base with hMGMT resulted in slow demethylation, but the addition of non-methylated DNA to the free base/hMGMT mixture restored the fast kinetics [13]. While there may be some subtle differences in repair rate depending on the surrounding sequence, it is clear MGMT repairs O^6MG in a variety of sequence contexts, as might be expected from a lesion that could occur anywhere in the genome [14-18]. Binding constant studies put dissociation constants (K_d) for MGMT-DNA complexes in the low (0.5-20) micromolar range for both methylated and unmethylated DNA [10,11,19-21]. This moderate affinity for DNA and low preference for methylated over unmethylated DNA in particular may be reflected in the low sequence specificity of repair.

As indicated above, the most highly studied MGMT proteins are hMGMT and AdaC. Although the proteins are equivalent in their overall function, some differences exist in their repair and binding characteristics. For instance, hMGMT is believed to bind cooperatively to DNA, while AdaC does not seem to [10,15]. In addition, hMGMT is inactivated by free O^6-benzylguanine (O^6BG), while AdaC is not. There are also differences in the rate of repair for different adducts by these proteins [12, 20]. Some of these differences reflect changes at the amino-acid sequence level; a tryptophan in AdaC located at an equivalent position as a serine in hMGMT prevents O^6BG from diffusing into the active-site and inactivating AdaC [21]. Other differences may reflect evolutionary changes in the way MGMT carries out its activity.

For example, the Ada protein is part of the adaptive response system in *E. coli.* Ada is a

two-domain protein; the 10kD N-terminal domain (AdaN) demethylates innocuous methylphosphotriesters with a cysteine residue, the 19kD C-terminal domain (AdaC) has MGMT activity. The adaptive response system appears to be a unique feedback mechanism within bacteria. Upon methylation, AdaN turns into a transcriptional activator of the Ada gene and other genes involved in DNA repair, including, AlkA, AlkB, and OGT (another protein with MGMT activity) [6]. Although there are feedback mechanisms for the induction of MGMT expression in human cells, only bacteria appear to have fused MGMT and a transcriptional activator [3,9,22]. The third branch of organisms, archaea, along with eukaryotes, contain the single domain MGMT protein. This is consistent with the idea that certain genes from archael sources resemble more their eukaryotic than prokaryotic counterparts [3,23].

MGMT is found in all branches of organisms, bacteria, archaea, and eukarya, emphasizing its importance in maintaining the integrity of the genome. Comparisons between the various branches are instructive about the processes that govern protein evolution and the different characteristics that determine reactivity. Here we report the first solution structure of an MGMT protein from the thermophilic organism *Methanococcus jannaschii*. Comparisons of the sequence, structure, and other characteristics of this protein, MJ1529, to other MGMT proteins whose structures have been solved are made. The structure of MJ1529 reveals a two-domain protein, highly similar in structure to hMGMT, AdaC, and MGMT from *Pyrococcus kodakarensis* (pMGMT) particularly in the domain known to be involved in DNA-binding, the C-terminal domain. The structure also reveals some areas of disorder in both the N and C-terminal domains, the latter which may have implications for how MGMT proteins recognize and accommodate lesions in DNA into the active-site.

RESULTS AND DISCUSSION

Although sequence homology strongly indicates that MJ1529 is an MGMT protein, the activity of the protein was verified in two ways. First, it is known that the addition of free O^6MG base to MGMT results in irreversible methylation of the protein [13]. Complete methylation of MJ1529 by this reaction was verified by mass spectrometry. Additionally, MJ1529 repaired O^6MG within double stranded oligonucleotides, as shown by a restriction endonuclease cleavage assay (see Experimental) [24].

The ^{1}H-^{15}N HSQC spectrum of MJ1529 is shown in Figure 2. The peaks are labeled with the one letter amino acid code and protein sequence number. All backbone amide resonances were assigned except for I24, S141, and the last 7 amino acids of the protein, which are structurally disordered. There are extra resonances in the HSQC that could not be assigned, some of which likely represent proteolysis products. Some residues gave weaker crosspeaks, these arise from amide protons in residues 60-65, 93-94, and 152-156 which are close to each other in space and are somewhat less well defined in the protein structure. This likely indicates some conformational flexibility in this region. The amide proton of E61 appears to shift in different spectra and a FHSQC spectrum taken with high resolution and signal to noise ratio revealed 3 weak peaks in the spectral region with E61. The amide peak of Tyr 140, a fully conserved residue in the C-terminal domain, is also weak and sidechain protons could not be unambiguously assigned for this residue. An example of data from a three dimensional spectrum acquired from ^{15}N labeled MJ1529 is shown in Figure 3.

All of the restraints included in structure calculations and the statistics of the lowest energy structures are shown in Table 1. In addition to NOE assignments, $J_{HN\text{-}H\alpha}$ couplings constants, dihedral angle restraints (from TALOS), hydrogen bonds, and residual dipolar couplings were used [25]. NOE assignment was aided by the automatic assignment programs

CYANA and ARIA. Final calculations incorporating residual dipolar couplings were performed using CNS [26-28].

An ensemble of the 10 lowest energy structures for MJ1529 is shown in Figure 4. The ensemble reveals that MJ1529 is a two-domain protein with an α/β fold. The N-terminal domain consists of a three-stranded antiparallel β sheet, β1– β3, a largely disordered region with some α–helical characteristics (helix a), and helix b. Overall, the N-terminus is somewhat less well defined than the C terminus of the protein. The turn between β1 and β2 two lacks long range contacts, and no assignments could be unambiguously made for residue I24, near the end of β3. The C terminal domain consists of helix c, helix d, helix e, helix f, helix g, β5, and β6. Helices d and e form a helix-turn-helix motif, a well-established DNA binding element. Between the helix-turn-helix region and the terminal helix is a "wing". The wing, or helix-turn-wing motif is a structural element also implicated in DNA binding [29,30].

The structure of MJ1529 can be compared to the structures of other MGMT proteins that have been solved by X-ray crystallography; AdaC (PDB entry 1sfe), hMGMT (in the unmethylated, methylated, and benzylated forms) (1eh6), and pMGMT (from the hyperthermophile *Pyrococcus kodakarensis*-1mgt) [21,31-33]. A structure based sequence alignment reveals that although there is very little sequence homology in the N-terminal domains of the proteins (even for the thermostable MJ1529 and pMGMT, which are 35% identical over 100 residues), all the structures reveal the 3 stranded antiparallel β sheet (Figures 5 and 6). In hMGMT, a zinc atom binds sidechains in β1, β3, and a loop, but no other metal ions have been observed or their presence inferred in the other structures [21]. β1 in MJ1529 is shorter than in the other structures and the sheet has a less pronounced roll. The region corresponding to the sheet

and the disordered region before the beginning of helix b has approximately 10 fewer residues than the corresponding region in pMGMT, reflecting the difference in their respective sequence lengths (167 vs. 174). The shortest MGMT proteins identified to date are also from thermostable organisms [34]. A putative MGMT protein from *Thermatoga maritima*, identified through a Blast search using the MJ1529 sequence, contains just 139 residues, with the alignment beginning at the start of helix b in MGMT [35].

The greatest topological differences in the structures occur after the β sheet. In both AdaC and pMGMT, the β sheet is followed by an alpha helix. No density is observed in that portion of hMGMT crystal structure [21,31-33]. In the structure of MJ1529, the region corresponding to this helix is largely disordered. Only a single amide proton, I31, is significantly protected from solvent exchange, compared to a much higher percentage of protection in other areas of secondary structure. HN-HN NOE cross peaks indicative of an α helix are observed for amides 29-35 as well as an NOE from amide of M35 to the H_α of F32, also indicative of helix formation. The integrity of the corresponding helix in pMGMT is maintained by 2 intra-helix ion pairs (salt links between sidechains of residues i and i+3/4) that span the rather long, 16 residue helix, and are speculated to contribute to the thermostability of the protein [33]. Comparison of the sequences of the two thermophiles reveals that MJ1529 has only one potential intra-helix ion pair (R27-E30), and this occurs in the transition from β3 to the disordered region. In addition, this region in MGMT is both shorter and more hydrophobic in nature. There are two phenylalanine residues, F32 and F34, for which only delta protons could be assigned due to the particularly high overlap of the phenylalanine aromatic protons. These residues are near I24, for which no assignments could be made, and it would seem likely these hydrophobic residues would interact. For those residues whose heteronuclear T2 values could be measured in this

region, R28, F34, D36, G37, D38, and V39 all had elevated values (> 0.3 s^{-1}) indicating this region may be dynamic. Following this region is helix b, which is oriented similarly in AdaC, MJ1529 and pMGMT, but lies at a slightly different angle in hMGMT.

It is not clear whether the N-terminal domain serves a biological function, but data indicate it contributes to structural stability. This is consistent with chemical shift mapping of DNA binding to AdaC, which reveals that few amide resonances shift in the N-terminal domain during DNA binding [19]. In addition, the lack of sequence conservation or length in the N-terminal domain (despite similar structural elements) also indicates it exists as a cap for the DNA-binding domain.

The C-terminal domains of the MGMT proteins are highly superimposable. This domain consists of helices d-g, β5, and β6. Superposition of this region of a minimized average structure of MJ1529 with pMGMT, AdaC, and hMGMT, shows a C_α RMSD of 1.8 Å (Figure 6.c). The similarity of these domains correlates with the higher level of sequence homology in this portion of the protein; all 19 of the absolutely conserved residues occur in the C-terminal domain (Figure 5). The sequence PCHRV, which contains the active-site cysteine, is the signature sequence that identifies potential MGMT proteins; all proteins identified as having MGMT activity contain this stretch of residues in their C-termini. Mutagenesis studies on these fully conserved residues implicate them in DNA-binding or active-site integrity [36,37]. As in the other MGMT structures, the active-site cysteine in MJ1529 is located in a 3_{10} helix, buried within the protein. It was first thought that MGMT underwent a substantial conformational change in order to place the cysteine in close enough contact to O^6 MG to repair it [32]. A much more elegant explanation, however, was derived from the studies of other DNA repair proteins, such as glycosylases and endonucleases. It was revealed through co-crystal structures of these proteins and DNA that

nucleotides could be "flipped-out" of the double helix into the active-site of the protein [38]. Support for this mode of repair by MGMT is provided by chemical shift mapping studies of AdaC, indicating that the structure is not greatly perturbed upon binding [19]. However, direct physical evidence for base-flipping by MGMT has been difficult to obtain due to the fast nature of the reaction.

A closer look at the C-terminal part of the protein reveals that the helix-turn-helix contains fully conserved residues Y99 (helix e) and R111, A112, and V113 (helix f) (Figure 6.d). For hMGMT a structural homology search using the DALI server identified the CAP (catabolite activating) protein as having the closest homology in its DNA-binding elements to MGMT [39]. A model of hMGMT bound to DNA based on the structure of the CAP protein bound to DNA indicates that helix f is the equivalent of the "recognition helix" that likely binds non-specifically in the major groove. In both MJ1529 and the crystal structures, R111 in helix f is exposed and in a position to interact with the negatively charged backbone of DNA. It is proposed that this invariant residue acts as an "arginine finger," injecting itself into the base stack and promoting the flipping out of the guanine base, and stabilizing the resulting structure, akin to other DNA repair enzymes that use amino acids to promote base-flipping [21,40-42]. A112 is proposed to make sequence-independent hydrophobic contacts with the DNA [21,31,38]. When the guanine is flipped into the active site, the hydroxyl of Y99 of helix e (whose mutation affects the reaction rate) is poised to form a hydrogen bond with the N3 of guanine. The small residues within the wing are proposed to make backbone hydrophobic contacts, in particular V131 and V132, while residues Y140 and S141 of the wing may also interact with the guanine. Invariant Y140 is shown to interact with the benzyl group of benzylated hMGMT [21].

The wing of MJ1529, particularly at the "level" of the active-site, is less-well defined

than other parts of the structure. No sidechain atoms could be positively assigned for the conserved Tyr 140, and its amide cross peak was weak in the HSQC. For the serine that follows it (present in all of the structures except AdaC), the amide proton could not be assigned. This is consistent with flexibility in this region. The corresponding region in pMGMT had increased B factors relative to the rest of the protein [33]. In AdaC, the equivalent residue to S141 shows significant changes in amide chemical shift upon titration with DNA. Other residues within the wing are also likely to interact with the DNA. Although not conserved, K134 is exposed at the tip of the wing, along with N135 and S136, and A133, which may make contacts with the DNA. A surface potential plot shows the charge complementarity of the recognition helix and wing with DNA (figure 7.a). Interaction of this region of the protein with DNA is consistent with chemical shift mapping data on AdaC, in which significant shifts of amide peaks upon titration with DNA occurred in helix e and helix f, and the wing residues (figure 7.b) [19, 33].

The active-site of MJ1529 is similarly constructed to those of the other structures. The sidechain of invariant H129 is in proximity to invariant E154 whose sidechain interacts with that of invariant R130 (Figure 7.c). It is proposed that this hydrogen bonding network results in deprotonation of C128, generating the nucleophile. One interaction that could not be detected (not likely due to its absence but due to data limitations) is a hydrogen bond between the sidechains of invariant N120 and C128. It is this interaction that is broken by alkylation, and results in a subtle structural change that destabilizes the protein, and in the case of hMGMT, signals the protein for ubiquitin dependent degradation [40].

The overall structure of MJ1529 is very similar to the structures of pMGMT, hMGMT, and AdaC. The largest differences occur in the N-terminal regions of the proteins where the secondary structural elements of MJ1529 are shorter than in the other protein structures, and

residues 29-39 are much less-structured than in pMGMT and AdaC. It is interesting to note, however, that the corresponding region in hMGMT is not present in the crystal structure, implying some flexibility in this region. Other possibly dynamic regions include residues 60-65, which have weak amide resonances, and do not superimpose well in the structure.

The C-terminal domains are all highly superimposable, as expected from the level of sequence conservation. In all of the structures, the active-site cysteine is buried within the protein, and invariant residues from the helix-turn-helix and wing are exposed and poised to interact with the DNA.

The two thermophilic proteins share many characteristics at the sequence level. These include helix capping by proline residues, the pattern of i, i+3/4 charged side-chain residues that are shown to form intra and inter-helix ion-pairs in the KOD structure, and a short deletion in the loop between helices e and f, all of which may contribute to the thermostability of the proteins [33].

EXPERIMENTAL

A clone of MJ1529 in pet21a (Novagen) was kindly provided by Hisao Yokota, and was transformed into BL21(DE3) pACYC cells. Transformants were grown in 2ml cultures of LB containing ampicillin and kanamyacin and used to inoculate 1 L of LB, 1 L of M9 with $^{15}NH_4Cl$ (^{15}N labeled), or 1 L of M9 with $^{15}NH_4Cl$ and ^{13}C glucose ($^{15}N/^{13}C$ labeled). 1 mg of thiamine and trace metals were added to M9 growths. Cells were grown to an O.D. of 0.6-0.8, whereupon 50 mgs/L of IPTG was added to induce expression. Cells were allowed to grow 5-6 hours more and harvested by centrifugation.

Harvested cells were resuspended in 50 mM Tris, pH 7.4, 50 mM NaCl, 3mM DTT and 200 μM PMSF, then were sonicated on ice and insoluble matter was spun down by high-speed centrifugation. The supernatant was placed in a 60-70° C water bath for approximately $^1/_2$ hour to

precipitate most *E. coli* proteins, then the solution was again centrifuged and the supernatant was applied to an SP Sepharose column, and washed extensively with 50mM Tris, 200 mM NaCl, until the detector absorbance returned to baseline levels. A salt gradient from 200 to 650 mM NaCl (300 mls total) was run, with MJ1529 eluting at approximately 450 mM NaCl. Typical yields were ~10 mg/L for LB and ~8mg/L for M9 preparations. The molecular weight of the purified protein was verified by mass spectrometry.

After the purification, MJ1529 was dialyzed into 50mM sodium phosphate buffer, pH 6.2, 500mM NaCl, 1mM DTT, and 0.02% NaN_3 and concentrated to 0.4-0.8 mM in Amicon centrifugal filters.

For the residual dipolar coupling experiments, the protein was dialyzed into a low salt buffer (25mM sodium phosphate, pH 6.7, 50mM NaCl or 200mM NaCl) before being diluted with bicelle stocks [50]. The resulting protein solutions were 150-250 μM but transferring assignments from different salt and different pH solutions was not difficult.

O^6 methylguanine was purchased from Sigma and incubated with MJ1529 overnight at 37° C. After reverse-phase HPLC, the protein was analyzed by mass spectrometry revealing that the protein had become fully methylated. During the reaction with the free O^6MG base, it was noted that protein precipitate formed, which agrees with the findings that MGMT proteins are destabilized by methylation [51].

To verify MGMT activity a single O^6-methylguanine lesion was incorporated within a double stranded piece of DNA containing multiple restriction endonuclease sites. The O^6-methylguanine containing strand was fluorescently labeled with 6-hexachlorofluorescein (HEX). The lesion was incorporated in the middle of a PVU II site (CAG*CTG), which cannot cleave if the central guanine is methylated. Thus, when the protein is incubated with the modified oligo,

the lesion is repaired and reaction with PVUII results in cleavage of the oligo which can be quantified by running the DNA on a gel and measuring the fluorescence [24].

The oligos were ordered (purified by HPLC) from Synthegen (Texas) and designed as follows, with the G* representing O^6-methylguanine: Hex-GCCCGGCCAG*CTGCAGCG with CGCTGCAGCTGGCCGGGC. The dried oligos were dissolved separately in 10mM Tris, pH 8, 33 mM NaCl, and 1mM EDTA. The oligos contained a PVUII site and an HAE III site used as an internal control. The fluorescently labeled oligo and an excess of the complementary oligo were combined and heated at 90° C for 2-3 minutes and then allowed to anneal at room temperature overnight. The subsequent solution was aliquoted and frozen at -20° C for further use. 10-20 pmols of the annealed oligo were incubated either without or with various concentrations of purified MJ1529 in 150 µls total volume of buffer containing 50 mM Tris, pH 7.4, 5% glycerol, and 1mM DTT. The reactions were incubated from 2-12 hours at 37° C, and for 2 hours at 55° C. The DNA was extracted by vortexing with an equal volume of phenol (50): chloroform (49): isoamyl alcohol (1) and keeping the aqueous layer (repeated twice), followed by chloroform (99): isoamyl alcohol (1) extraction. To the retained fraction 150 µl of 0.5M NaOAc pH 5 was added, followed by 25-30 µl of 1mg/ml tRNA, to help precipitation of the DNA. To this mixture, 0.3 ml of cold 100% ethanol was added and the mixture was allowed to sit overnight at –20° C. The following day the ethanol mixture was spun in a microcentrifuge at 13k rpm for 4 minutes and the ethanol was poured off. The pellet was dried in a speed vacuum and then redissolved in 20 µls buffer appropriate for incubation with PVUII or HAE III. The restriction endonuclease reactions were allowed to proceed for 1-2 hours, stopped with 10 µls formamide (containing 20 mM EDTA), and heated at 95° C for 5 minutes to separate the DNA

strands, and then loaded on a prerun 20% acrylamide gel containing 7M Urea in TBE buffer. The gels were imaged with a Typhoon Fluoroimager using excitation of the HEX oligo at 535 nm and emission at 556 nm. The assay results reveal that MJ1529 does repair O^6-methylguanine within double stranded oligonucleotides.

NMR experiments were performed on Bruker AMX-600, DRX-500, or DRX-500 (with a cryoprobe for residual dipolar coupling experiments) spectrometers. Experiments were performed at 30° C, unless otherwise noted. Interresidue connectivity was established by analysis of HNCA [53], CBCA(CO)NH [54], ^{15}N edited NOESY-HSQC [55], HBHA(CO)NH [56], and ^{15}N edited TOCSY-HSQC [57] spectra with Watergate for solvent suppression [55]. Intraresidue connections were identified using ^{15}N edited NOESY-HSQC, ^{15}N edited TOCSY-HSQC, and ^{13}C edited HCCH TOCSY [58] (D_2O) spectra. Carbonyl carbons were assigned with an HNCO experiment. $^3J_{NH\alpha}$ coupling constants were determined by peak intensity analysis of an HNHA experiment [59] and converted to coupling restraints in the program NMRVIEW [60]. Hydrogen bonds were inferred from analysis of secondary structure indicated by HN-HN connections in the ^{15}N edited NOESY-HSQC, and D_2O- exchange experiments in which the protein solution was lyophilized and redissolved in 100% D_2O, and monitored by successive Fast ^{1}H-^{15}N HSQC (FHSQC) experiments for the next several hours [61]. Peaks that had a long lifetime were inferred to be involved in hydrogen bonds, and when consistent with other secondary structural indications, were used as restraints during structure calculations.

Aromatic resonances were assigned using a ^{1}H-^{1}H NOESY on labeled protein, ^{1}H-^{1}H TOCSY, ^{15}N edited NOESY-HSQC, 4D HMQC-NOE (D_2O), and aromatic ^{1}H-^{13}C HSQC spectra (CT-HSQC, HMQC, etc.) [62,63]. Due to high degeneracy in the chemical shifts of the phenylalanine aromatic protons and carbons, a ^{13}C-^{15}N labeled, ^{12}C, ^{14}N-labelled phenylalanine

sample was made by introducing unlabelled phenylalanine to a minimal media growth (known as reverse isotopic labeling). Using this strategy, only tyrosine and histidine signals are found in the aromatic region of spectra relying on ^{13}C-labelling. Analogously, ^{12}C- filtered experiments will only yield signals from phenylalanine, without the line-broadening associated from proton attachment to isotopically labeled carbons [63]. 2D CT-HSQC, 2D-HMQC, and 3D ^{13}C NOESY spectra were run, placing the carrier at 125 ppm to maximize the aromatic contributions to the spectra. At least a delta proton resonance for each phenylalanine was assigned. A 1D of the aromatic region verified the extent of the overlap and also some broad peaks, indicating the presence of some dynamic regions of the protein, consistent with the structure presented here. Two of the phenylalanines, F32 and F34, are in a largely unstructured portion of the protein, as are aromatic residues after residue 160. Stereospecific assignments of methyl groups were generated by making a 10% labeled ^{13}C sample and running a CT-HSQC experiment [64,65].

NMR data were processed on Silicon Graphics Indigo2 workstations using Felix 97 or NMRPipe [66], and visualized using the program NMRVIEW. The chemical shift indexing in NMRVIEW was helpful for identifying secondary structure [68]. Peak lists for all spectra were either generated with the peak picking algorithm incorporated in NMRVIEW or with the program PIPP [67].

For the four dimensional NOESY data from the ^{13}C/^{13}C HMQC-NOE [69] and ^{15}N/^{13}C (HMQC/HSQC) NOE [70] some peaks were assigned manually. An in-house program listing possible assignments according to chemical shifts was used to generate possible assignments for each peak. Initial structures were generated (3-5 Å RMSD) and were used to distance filter probable assignments (possibilities were eliminated if they were > 8 Å apart in the structures). This approach led to some assignments, but the low quality of the initial structures made this

process difficult; thus, distance filtering was also done through examination of homologous structures. Using sequence alignment and comparison of regions of secondary structure, peak filtering for MJ1529 was done using the structure from *Pyroccocus kodakarensis*, the most homologous protein [33].

As described above, initial restraints were generated from manual assignment of 3D ^{15}N-NOESY and partial assignment of 4D ^{13}C/^{13}C and ^{15}N/^{13}C NOESYs. These restraints were incorporated into structure calculation using the program DYANA [71]. In addition, $^{3}J_{\mathrm{HN\text{-}H\alpha}}$ coupling constants providing information on ϕ dihedral angles were used as restraints. The program TALOS was used to generate a list of likely phi and psi dihedral angles based on comparison of sequence triplets to a database containing structure and sequence information from the RCSB [25]. 100 structures were generated, and the 20 with lowest energy were analyzed for consistent NOE distance violations. This yielded structures with an overall RMSD of ~2.5Å.

To aid NOE assignment, the programs ARIA and CYANA, which both incorporate ambiguous NOE's into structure determination as part of an iterative assignment process, were used [26-28]. Although in principle each program may be used *de novo*, i.e. without any initial structures or restraints, it was found that providing initial structures from manual assignments (including NOE's, coupling constants, and hydrogen bonds) greatly improved the success of the assignment process for both programs. After the runs, unambiguous, ambiguous, and rejected peak lists were inspected for accuracy. Although many assignments appeared to be correct, some accepted peaks were incorrectly assigned, while some ambiguous assignments that were rejected based on stringent criteria, were reincorporated in the structure calculation process.

Results from ARIA yielded a highly converged C-terminus (for residues 70-140, the overall RMSD was 0.9 Å.) However, almost no structure was detected at all by the program in

the N-terminal part of the protein, and the C-terminal helix was distorted due to improperly determined contacts with the N-terminus. The program CYANA, with similar initial inputs as ARIA, yielded a clearly discernable three stranded β-sheet in the N-terminal part of the protein and resulted in an overall RMSD for residues 3-25, and 48-155 of 1.5 Å.

Through manual and automated assignment by ARIA and CYANA, approximately 1000 NOE distance restraints (binned either automatically by the above programs or through the program NMRVIEW) were determined. Although there is some inherent "unstructuredness" to the protein, particularly in the N-terminus, residual dipolar coupling (rdc) data was acquired to provide more long-range orientational restraints.

The final residual dipolar coupling data used in structure calculations of MJ1529 were derived from a sample containing 25mM NaPhos, 200mM NaCl, and 5% DMPC:DHPC:CTAB (30:10:1 molar ratio.)[72] (AVANTI Polar Lipids.) After temperature induced alignment, 2D IPAP-HSQC spectra were acquired 312 K [73]. Isotropic spectra were acquired at 303 K. This data resulted in 71 HN-N rdc's being incorporated into structure calculations. A modified HNCO experiment was used to measure C^{α}-C' couplings, and a SEMI-CT-HSQC was acquired to extract HN-C', and N-C' couplings simultaneously [74]. Although the addition of CTAB enhanced the stability of the sample over undoped bicelles, deterioration of the sample over time was noticeable.

For determining the magnitude and rhombicity of the alignment tensor, a histogram of the measured dipolar couplings was plotted, yielding an approximate D_a and R by analysis of the distribution [75]. This last method relies upon a uniform distribution of couplings (and hence bond vectors) and the accuracy improves as more types of rdc data are added. Histograms of the data yielded by study of MJ1529 did not resemble a powder pattern. The maximum values of Da

were different in different experiments, meaning that there was either non-uniformity in the distribution of couplings, or that the alignment tensor was changing over time due to inherent instability of the sample. Thus, rough estimates of Da and R were refined according to the procedure of Clore, *et al*.[76] . Residual dipolar couplings were incorporated into the program CNS as restraints with the alignment tensor being represented as a pseudo-four atom molecule. Given the difficulty in data acquisition and analysis, only data from one type of bond vector were used (HN-N) and the force constant was set to a relatively low value (0.3 kcal/Hz^2). The final Da and R values used were -7.0 Hz and 0.30, respectively. Residual dipolar coupling data was used in the refinement of initial structures calculated without residual dipolar couplings. The annealing protocol included 2000 slow cooling torsion angle dynamics steps, and 6000 additional Cartesian dynamics steps.

CONCLUSIONS

Protein/DNA interfaces are proposed to be somewhat flexible [19,44,45]. This would seem to be particularly important for DNA-repair proteins such as MGMT, that have little sequence specificity, little preference for double over single-stranded DNA, and can accommodate different sizes and types of base modifications. In the case of MGMT, this flexibility is likely to come from the wing portion of the protein. The broadening of some amide residues within the wing may indicate a conformational flexibility that allows the wing to adjust or move to allow the proposed extrahelical base to be exposed to C128 and other conserved residues in the active-site. This is more likely than flexibility within the helix-turn-helix, which is tightly coupled and constrained by secondary structure order.

One of the most intriguing questions that remains about MGMT is how it locates damaged bases among scores of unmodified bases. Studies of O^6MG containing

oligonucleotides indicate that the lesion is destabilizing (as judged by melting temperature), but otherwise causes only slight deformations in the backbone of DNA [46,47]. While it is possible that these modified bases are occasionally already extrahelical when MGMT comes along, other proposed methods of action by MGMT include processive movement along DNA by cooperative interactions between proteins, and targeting of MGMT to active-replication sites [20,48]. The NMR structures presented here may provide a basis to address such issues together with other biophysical studies.

REFERENCES

1. Vassylyev DG, Morikawa K. *Curr. Op. Struc. Bio.* 1997; **7**: 103.
2. Verdine GL, Bruner SD. *Chem. Biol.* 1997; **4**: 329.
3. Eisen JA, Hanawalt PC. *Mut. Res*. 1999; **435**: 171.
4. Bignami M, O'Driscoll M, Aquilina G, Karran P. *Mut. Res*. 2000; **462**: 71.
5. Kleibl K. *Mut. Res*. 2002; **512**: 67.
6. Lindahl T, Sedgwick B, Sekiguchi M, Nakabeppu Y. *Ann. Rev. Biochem*. 1988; **57**: 133.
7. Demple, B., In *Protein Methylation*, Paik, WS, Kim, S (eds), CRC Press: Boca Raton, Fl, 1990; 285.
8. Lips J, Kaina B. *Mut. Res.* 2001; **487**: 59.
9. Pegg AE. *Mut. Res*. 2000; **462**: 83.
10. Takahashi M, Sakumi K, Sekiguchi M. *Biochem*. 1990; **29**: 3431.
11. Chan CL, Wu Z, Ciardelli T, Eastman A, Bresnick E. *Arch. Biochem. Biophys*. 1993; **300**: 193.
12. Spratt TE, Wu JD, Levy DE, Kanugula S, Pegg AE. *Biochem*. 1999; **38**: 6801.
13. Goodtzova K, Crone TM, Pegg AE. *Biochem*. 1994; **33**: 8385.
14. Bender K, Federwisch M, Loggen U, Nehls P, Rajewsky MF. *Nuc. Acids Res*. 1996; **24**: 2087.

15. Fried MG, Kanugula S, Bromberg JL, Pegg AE. *Biochem*. 1996; **35**: 15295.

16. Liem L-K, Wong C-W, Lim A, Li BFL. *J. Mol. Bio.* 1993; **231**: 950.

17. Dolan EM, Oplinger M, Pegg AE. *Carcinogenesis*. 1988; **9**: 2139.

18. Delaney JC, Essigmann JM. *Biochem*. 2001; **40**: 14968.

19. Verdemato PE, Brannigan JA, Damblon C, Zuccotto V, Moody PCE, Lu-yun L. *Nuc. Acids Res*. 2000; **28**: 3710.

20. Rasimas JJ, Pegg AE, Fried MG. *J. Biol. Chem.* 2003; **278**: 7973.

21. Daniels DS, Mol CD, Arvai AS, Kanugula S, Pegg AE, Tainer JA. *EMBO*. 2000; **19**: 1719.

22. Grombacher T, Eichhorn U, Kaina B. *Oncogene*. 1998; **17**: 845.

23. Bult CJ, White O, Olsen GJ, Zhou L, Fleischmann RD, Sutton GG, Blake JA, FitzGerald LM, Clayton RA, Gocayne JD, Kerlavage AR, Dougherty BA, Tomb JF, Adams PD, Reich CI, Overbeek R, Kirkness EF, Weinstock KG, Merrick JM, Glodek A, Scott JL, Geoghagen NS, Venter JC. *Science*. 1996; **273**: 1058.

24. Kreklau EL, Limp-Foster M, Liu N, Xu Y, Kelley MR, Erickson LC. *Nuc. Acids Res*. 2001; **29**: 2558.

25. Cornilescu G, Delaglio F, Bax A. *J. Biomol. NMR*. 1999; **13**: 289.

26. Brunger AT, Adams PD. *Acta Crystall. D*. 1998; **54**: 905.

27. Herrmann T, Guntert P, Wuthrich K. *J. Mol. Bio*. 2002; **319**: 209.

28. Linge JP, O'Donoghue SI, Nilges M. *Meth. Enz*. 2001; **339**: 71.

29. Wintjens R, Rooman M. *J. Mol. Bio.* 1996; **262**: 294.

30. Vora RA, Pegg AE, Ealick SE. *Prot: Struct., Func., Gen.* 1998; **32**: 3.

31. Wibley JEA, Pegg AE, Moody PCE. *Nuc. Acids Res*. 2000; **28**: 393.

32. Moore MH, Gulbis JM, Dodson EJ, Demple B, Moody PCE. *EMBO.* 1994; **13**: 1495.

33. Hashimoto H, Inoue T, Nishioka M, Fujiwara S, Takagi M, Imanaka T, Kai Y. *J. Mol. Bio*. 1999; **292**: 707.

34. Skorvaga M, Raven NDH, Margison GP. *Proc. Natl. Acad. Sci., USA*. 1998; **95**: 6711.

35. Altschul SF, Gish W, Miller W, Myers EW, Lipman DJ. *J. Mol. Biol*. 1990; **215**: 403.

36. Pieper RO, Morgan SE, Kelley MR. *Carcinogenesis*. 1994; **15**: 1895.

37. Goodtzova K, Kanugula S, Edara S, Pegg AE. *Biochem*. 1998; **37**: 12489.

38. Roberts RJ, Cheng X. *Ann. Rev. Biochem.*. 1998; **67**: 181.

39. Holm L, Sander C. *J. Mol. Bio*. 1993; **233**: 123.

40. Daniels DS, Tainer JA. *Mut. Res*. 2000; **460**: 151.

41. Lau A, Scharer OD, Samxon L, Verdine GL, Ellenberger T. *Cell*. 1998; **95**: 249.

42. Slupphaug G, Mol CD, Kavli B, Arvai AS, Krokan HE, Tainer JA. *Nature*. 1996; **384**: 5105.

43. Schultz SC, Shields GC, Steitz TA, *Science*. 1991; **253**: 1001.

44. Kalodimos CG, Bonvin AMJJ, Salinas RK, Wechselberger R, Boelnes R, Kaptein R. *EMBO*. 2002; **21**: 2866.

45. Slijper M, Boelnes R, Davis AL, Konings RNH, van der Marel GA, Van Boom JH, Kaptein R. *Biochem*. 1997; **36**: 249.

46. Patel D, Shapiro L, Kozlowski SA, Gaffney BL, Jones RA. *Biochem*. 1986; **25**: 1027.

47. Gaffney BL, Jones RA. *Biochem*. 1989; **28**: 5881.

48. Ali RB, Teo AK-C, Oh H-K, Chuang LS-H, Ayi T-C, Li BFL. *Mol. Cell. Bio.* 1998; **18**: 1660.

49. Wong KB, Lee CF, Chan SH, Leung TY, Chen YW, Bycroft M. *Prot. Sci.* 2003; **12**: 1483.

50. Ottiger M, Bax A. *J. Biomol NMR*. 1998; **12**: 361.

51. Kanugula S, Goodtzova K, Pegg AE. *Biochem. J*. 1998; **329**: 545.

52. Leclere MM, Nishioka M, Yuasa T, Fujiwara S, Takagi M, Imanaka T. *Mol. Genes Gen*. 1998; **258**: 69.

53. Grzesiek S, Bax A. *J. Mag. Res.*. 1992; **99**: 201.

54. Grzesiek S, Bax A. *JACS*. 1992; **114**: 6291.

55. Sklenar V, Piotto M, Leppik R, Saudek V. *J. Mag. Res. A*. 1993; **102**: 241.

56. Grzesiek S, Bax A. *J. .Biomol. NMR*. 1993; **3**: 185.

57. Cavanagh J, Rance M. *J. Mag. Res*. 1992; **96**: 670.

58. Kay LE, Xu G-Y, Singer AU, Muhandiram DR, Forman-Kay JD. *J. Mag. Res. B*. 1993; **101**: 333.

59. Kuboniwa H, Grzesiek S, Delaglio F, Bax A. *J. Biomol. NMR*. 1994; **4**: 871.

60. Johnson BA, Blevins RA. *J. Biomol. NMR*. 1994; **4**: 603.

61. Mori S, Abeygunawardana C, Johnson M, Vanzijl PCM. *J Mag. Res. B*. 1995; **108**: 94.

62. Santoro J, King GC. *J Mag. Res*. 1992; **97**: 202.

63. Vuister GW, Kim S-J, Wu C, Bax A. *JACS*. 1994; **116**: 9206.

64. Neri D, Szyperski T, Otting G, Senn H, Wuthrich K. *Biochem*. 1989; **28**: 7510.

65. Johnson PE, Joshi MD, Tomme P, Kilburn DG, McIntosh LP. *Biochem*. 1996; **35**: 14381.

66. Delaglio F, Grzesiek S, Vuister GW, Zhu G, Pfeifer J, Bax A. *J. Biomol. NMR*. 1995; **6**: 277.

67. Garrett DS, Powers R, Gronenborn AM, Clore GM. *J. Mag. Res.* 1991; **95**: 214.

68. Kuszewski J, Qin J, Gronenborn AM, Clore GM, *J. Mag. Res. B*, 1995; **106**: 92.

69. Vuister GW, Clore GM, Gronenborn AM, Powers R, Garrett DS, Tschudin R, Bax A. *J. Mag. Res. B*. 1993; **101**: 210.

70. Kay LE, Clore GM, Bax A, Gronenborn AM. *Science*. 1990; **249**: 411.

71. Guntert P, Mumenthaler C, Wuthrich K. *J. Mol. Bio*. 1997; **273**: 283.

72. Losonczi JA, Prestegard JH. *J. Biomol. NMR*. 1998; **12**: 447.

73. Ottiger M, Bax A. *J. Mag. Res*. 1998; **131**: 373.

74. Ottiger M, Bax A. *JACS*. 1998; **120**: 12334.

75. Clore GM, Gronenborn AM, Bax A. *J. Mag. Res.*, 1998; **133**:216.

76. Clore GM, Gronenborn AM, Tjandra N. *J. Mag. Res.*, 1998; **131**: 159.

77. Koradi R, Billeter M, Wuthrich K. *J. Mol. Graph.* 1996; **14**: 51.

78. Kraulis EA. *J. App. Cryst*. 1991; **D50**: 869.

79. Merritt EA, Bacon DJ. *Meth. Enz*. 1997; **277**: 505.

80. DeLano WL, *The Pymol Mol. Graph. Sys*. DeLano Scientific, San Carlos, CA, 2002.

Table 1

Statistics for Structure Calculation of MJ1529

Conformational Restraints	
Total NOE Restraints	1023
Intraresidue	207
Short (|i-j| =1)	300
Medium Range (1< |i-j| <5)	296
Long Range (i-j| ≥5)	250
Hydrogen Bond Restraints	105
$^{3}J_{HN-H\alpha}$ Coupling Constants	101
Dihedral Angle Restraints	114
ϕ	58
ψ	56
Residual Dipolar Couplings	
HN-N	71
Residual Violations	
r.m.s deviation from experimental restraints	
Distance Violations (#/rmsd in Å)	0/0.022
Dihedral Angle (°)	0.221
Coupling Constants (Hz)	0.600
HN-N rdc's	3.17
r.m.s deviation from idealized geometry	
Bonds (Å)	0.0022
Angles (Å)	0.37
Impropers (Å)	0.23
Backbone RMSD	
Residues 2-155	1.40 Å
Ordered Structure (3-25, 48-60, 65-130,145-155)	1.02 Å
DNA-Binding Domain (80-155)	0.90 Å
Procheck Statistics (ordered regions 3-25,48-155)	
Most Favored	64.0
Additionally Allowed	31.9
Disallowed	4.1

Figure Captions:

Figure 1 Altered base-pairing of O^6 methylguanine that results in a GC→AT mutation during replication.

Figure 2 ^{1}H-^{15}N HSQC spectrum of MJ1529. The peaks are labeled with the one letter amino acid code and sequence number. Gray peaks are folded. Sidechain amides are connected by lines.

Figure 3 Strip plot showing the NOE connections between residues 102-105 in an ^{15}N resolved 3D NOESY. The arrows in black are represent HN-HN NOE's, typical of alpha helical regions. The arrows in gray show HN-aliphatic NOE's.

Figure 4 (a) Lowest energy ensemble overlay of MJ1529. The N-terminal domain contains a largely disordered region between residues 29 and 39 (b) Stereoview of the ordered regions (residues 3-25, 48-155) of MJ1529 (c) 90° rotation of (b) (structures were generated with MOLMOL [77]).

Figure 5 Structure based sequence alignment of MJ1529 from *Methanococcus jannaschhii*, MGMT from *Pyrococcus kodakarensis* (KOD), *Homo sapiens* (hMGMT), and *E. coli* (AdaC). Sheets are shown in rectangles, helices in rounded rectangles. The disordered region of MJ1529 is partially represented by a squiggly line. Similar residues are highlighted in bold, completely conserved residues are noted with a *. The active-site cysteine is shown is in the black highlighted box.

Figure 6 (a) Overlay of the N-terminal domains of a minimized averged structure of MJ1529 (yellow), hMGMT(red), pMGMT (blue), and AdaC (green). Helix a in MJ1529 is largely disordered. The Zinc atom of hMGMT is represented by a red sphere. (b) Overlay of the β–sheets, colored similarly to (a). The lengths of the strands vary, and the sheet has a pronounced roll (figures made with MOLSCRIPT and Raster3d [78-79]). (c) Superposition of the C-terminal domains of an average Mj1529 structure (yellow), pMGMT (blue), AdaC(green) and hMGMT (red.) The arrow indicates the active-site 3_{10} helix and the location of the cysteine. (d) ribbon diagram of the C-terminal domain of MJ1529 with fully conserved residues labeled with a *, which are speculated to be involved in DNA or form part of the active-site (generated with Pymol [80]).

Figure 7 (a) charge potential surface plot of MJ1529, positive charge is in blue, negative in red (b) DNA-binding domain of MJ1529 with the same orientation as in (a) with double-stranded DNA modeled in based on the CAP-DNA complex [43,80]. The wing residues are likely to shift to accommodate the flipping out of the base into the active-site. (c) Ribbon diagram of MJ1529. The helix-turn-helix is show in green, the wing in magenta. Conserved residues C128, H129, R130 and E154, composing part of the active-site network, are also shown.

Figure 1.

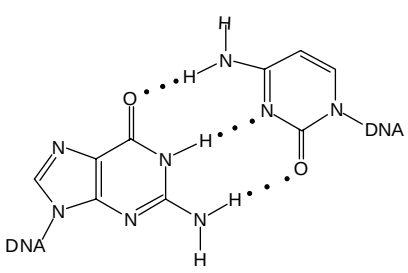

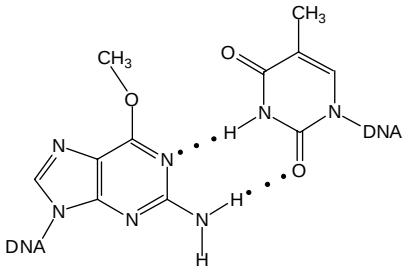

GUANINE **CYTOSINE** **O^6-METHYLGUANINE** **THYMINE**

Figure 2.

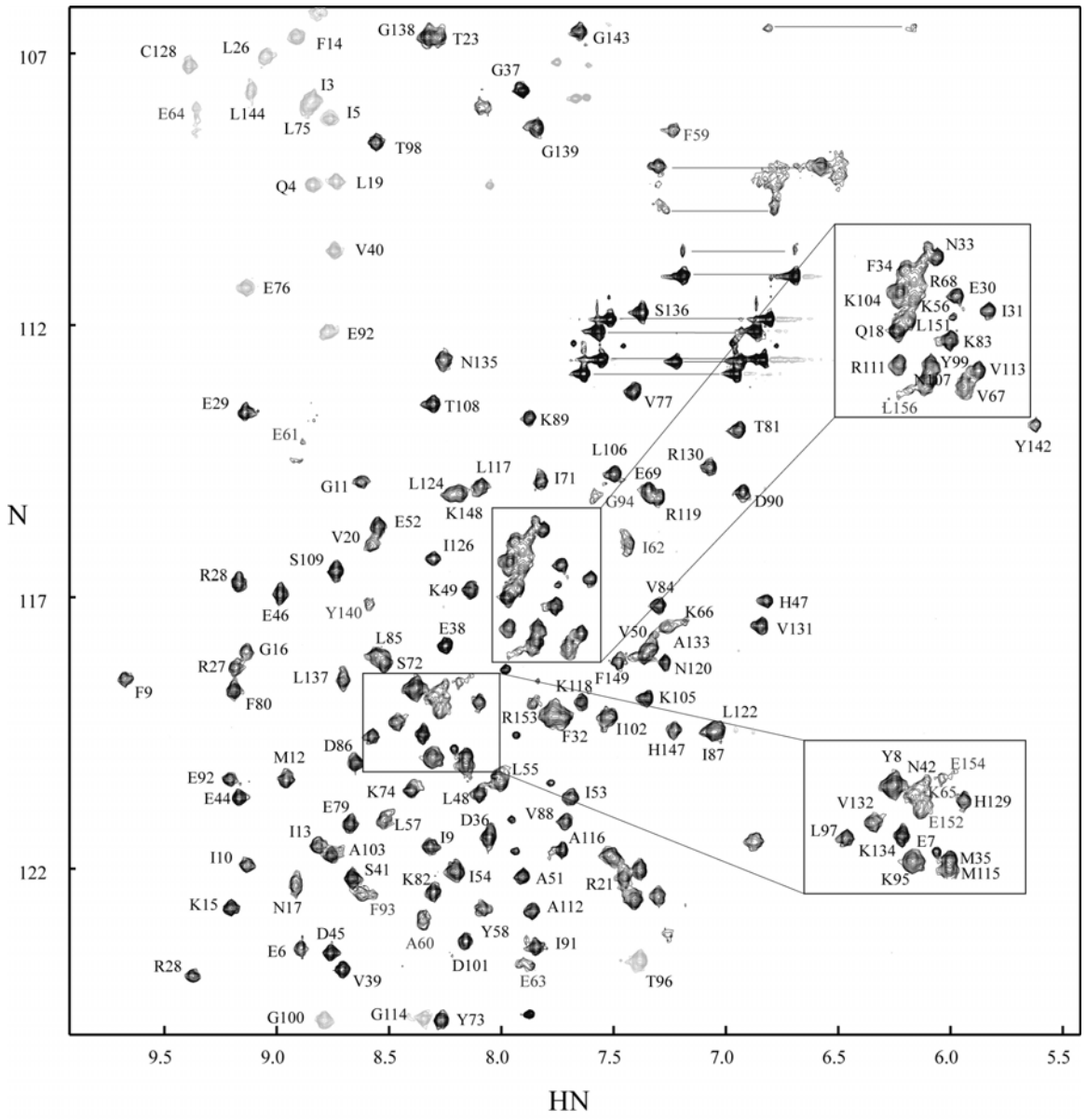
N
HN
107
112
117
122
9.5
9.0
8.5
8.0
7.5
7.0
6.5
6.0
5.5
C128
L26
F14
G138
T23
G143
G37
I3
E64
L144
L75
I5
T98
G139
F59
Q4
L19
V40
E76
E92
S136
N135
E29
T108
K89
V77
T81
Y142
E61
L106
R130
L117
L124
I71
E69
G11
G94
D90
K148
R119
E52
V20
I126
I62
S109
R28
K49
V84
H47
E46
Y140
K66
E38
V50
V131
L85
A133
G16
S72
N120
R27
L137
F149
K118
K105
F9
F80
R153
L122
F32
I102
H147
I87
D86
M12
L55
E92
K74
L48
I53
E44
E79
V88
D36
L57
I9
A116
I13
A103
I10
S41
K82
I54
A51
R21
K15
N17
F93
A112
D45
A60
Y58
I91
E6
D101
E63
T96
R28
V39
G100
G114
Y73
N33
F34
R68
E30
K104
K56
I31
Q18
L151
K83
R111
Y99
V113
N107
V67
L156
Y8
N42
E154
K65
H129
V132
E152
L97
E7
K134
M35
K95
M115

Figure 3.

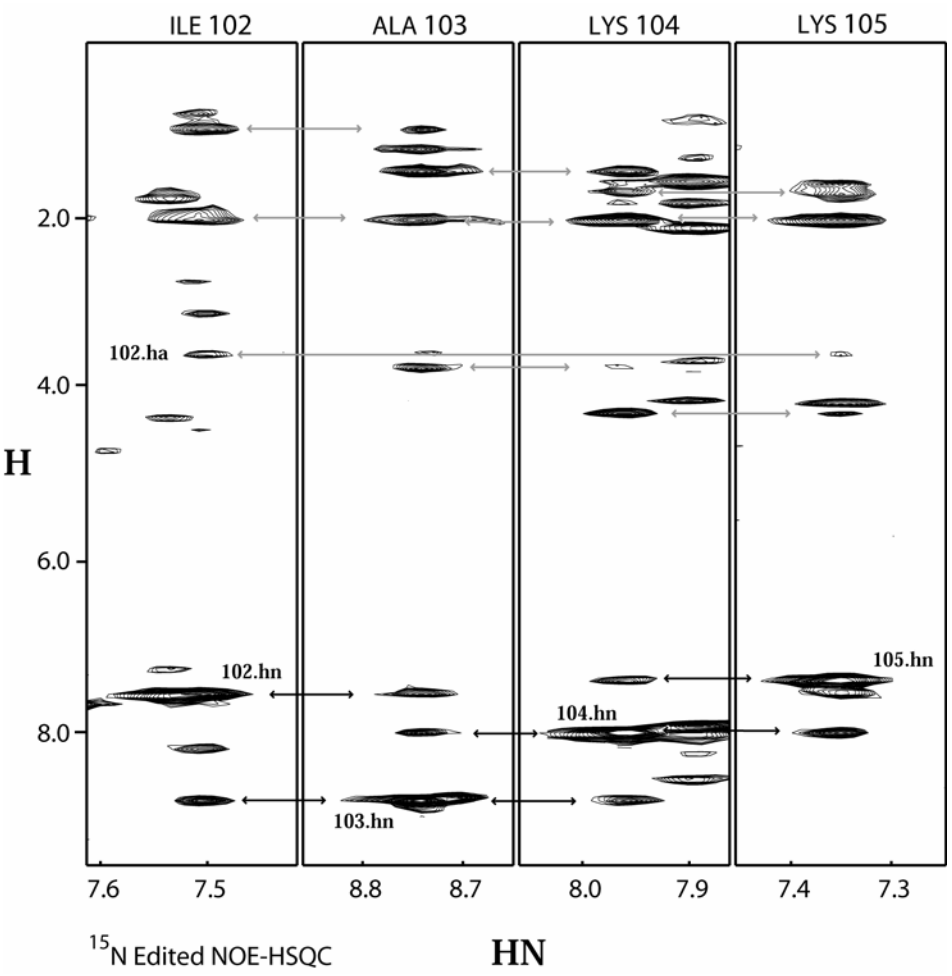
ILE 102
ALA 103
LYS 104
LYS 105
2.0
4.0
6.0
8.0
H
102.ha
102.hn
103.hn
104.hn
105.hn
7.6
7.5
8.8
8.7
8.0
7.9
7.4
7.3
15N Edited NOE-HSQC
HN

Figure 4.

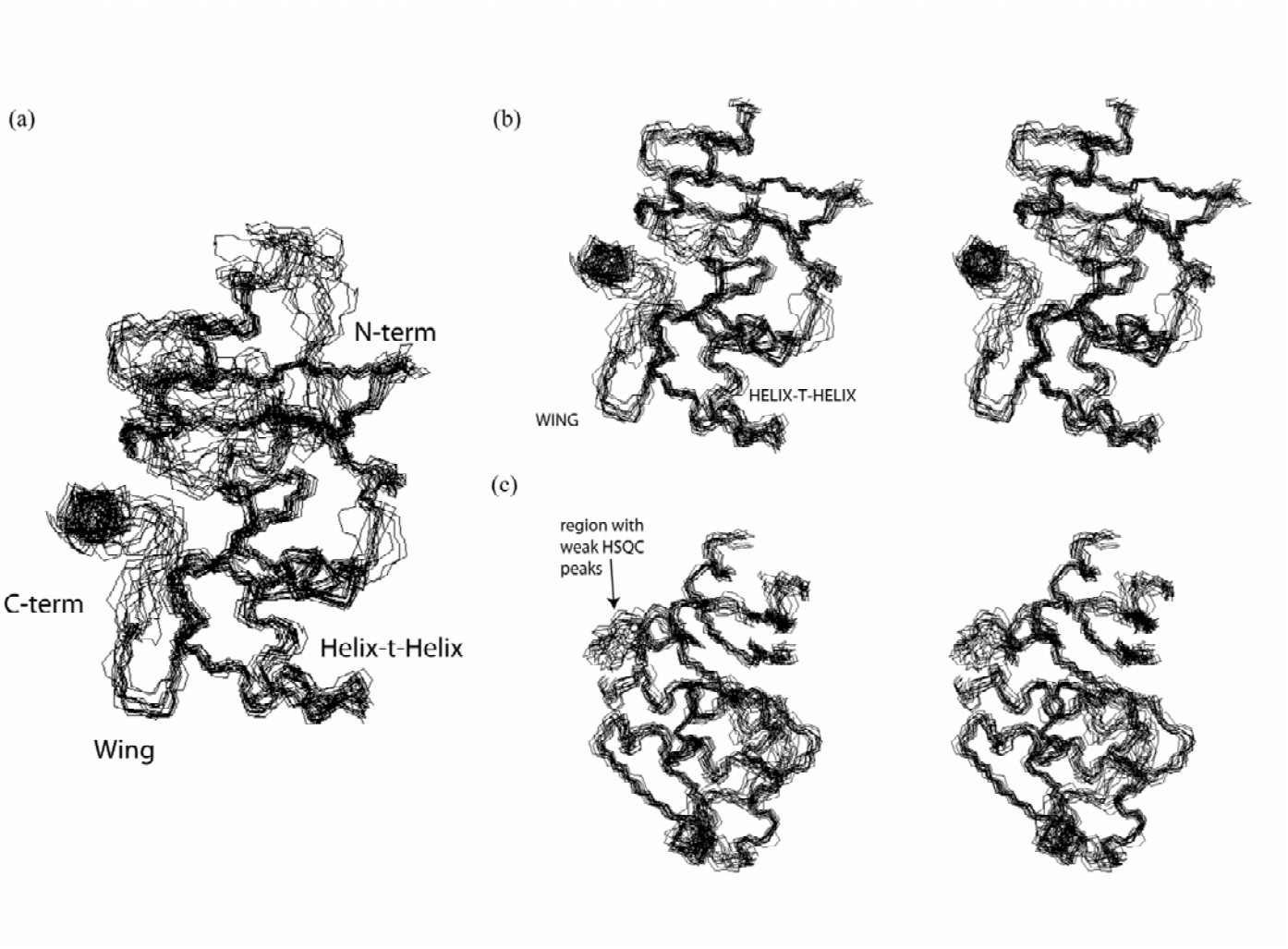
(a)
N-term
C-term
Helix-t-Helix
Wing
(b)
WING
HELIX-T-HELIX
(c)
region with
weak HSQC
peaks

Figure 5.

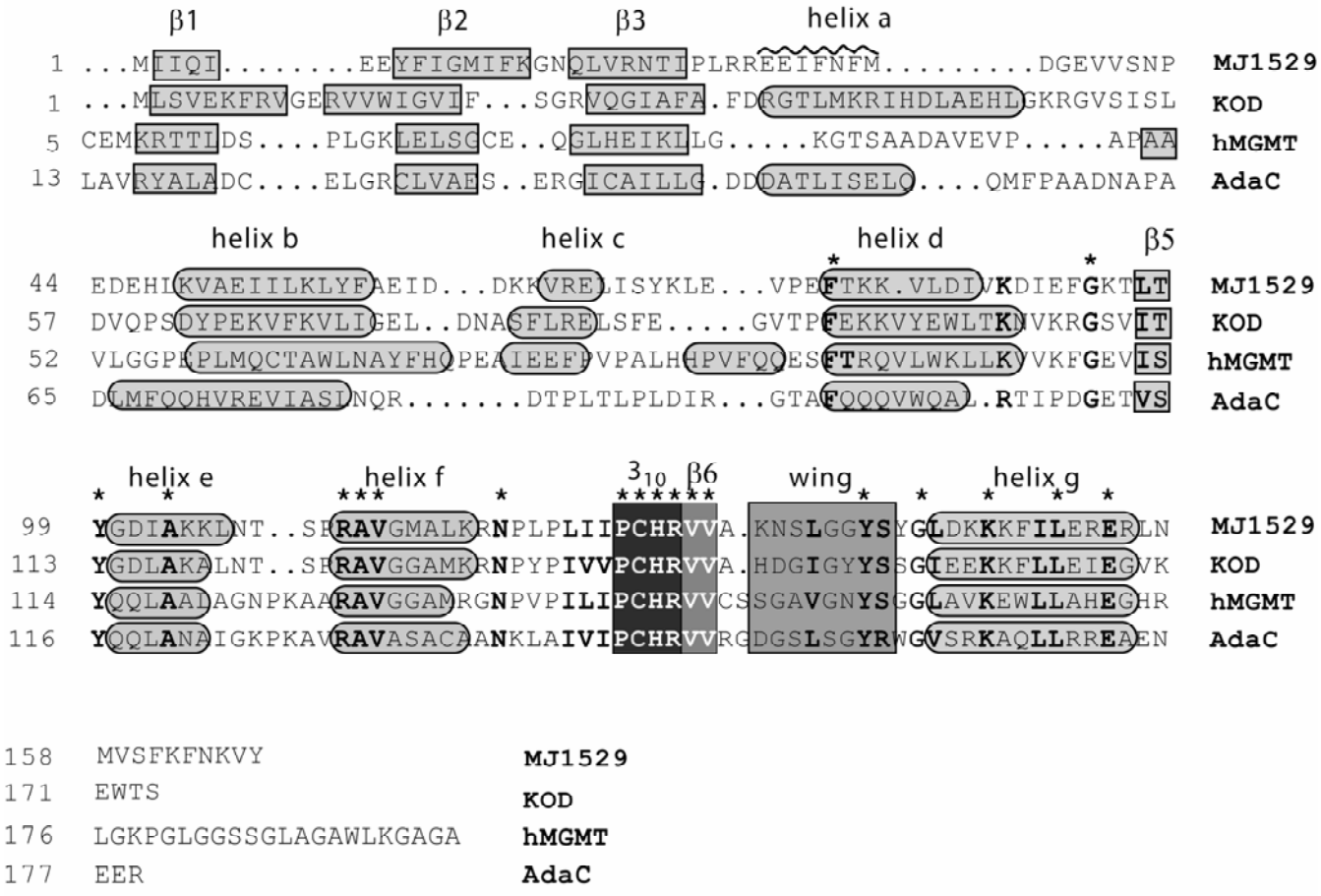
β1
β2
β3
helix a
MJ1529
KOD
hMGMT
AdaC
helix b
helix c
helix d
β5
helix e
helix f
3_{10}
β6
wing
helix g

Figure 6.

(a)

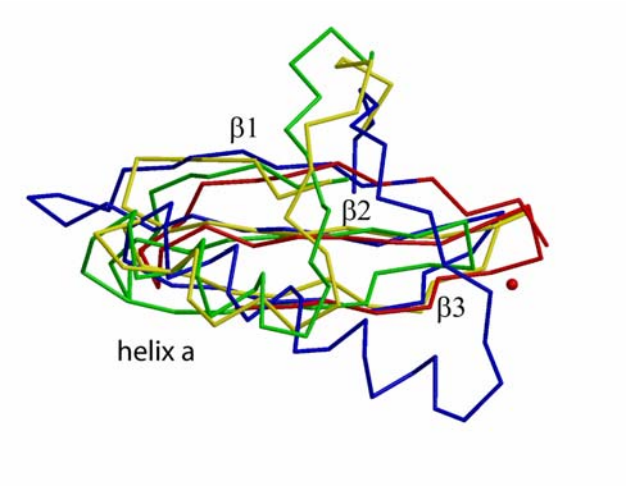

(c)

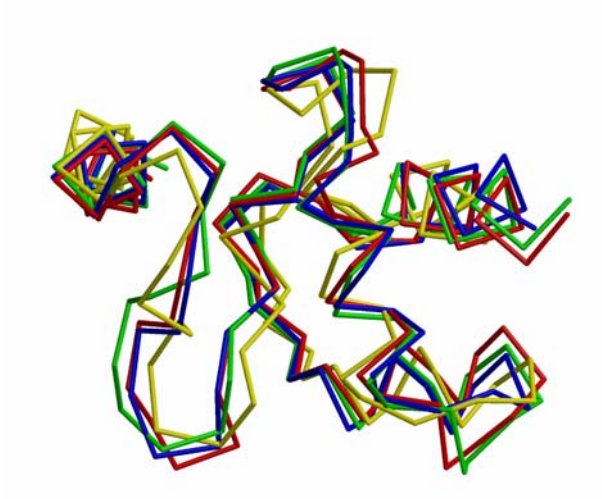

(b)

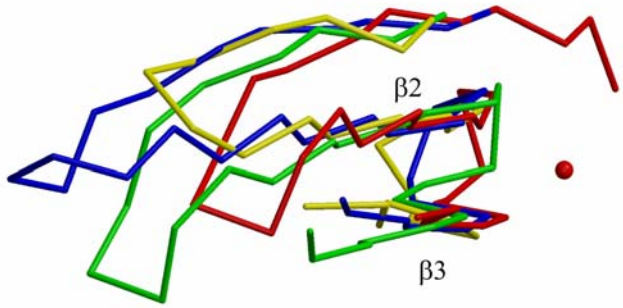

(d)

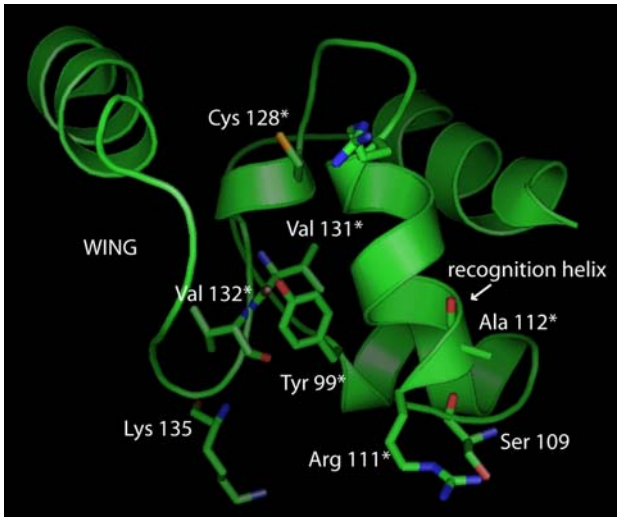

Figure 7.

(a)

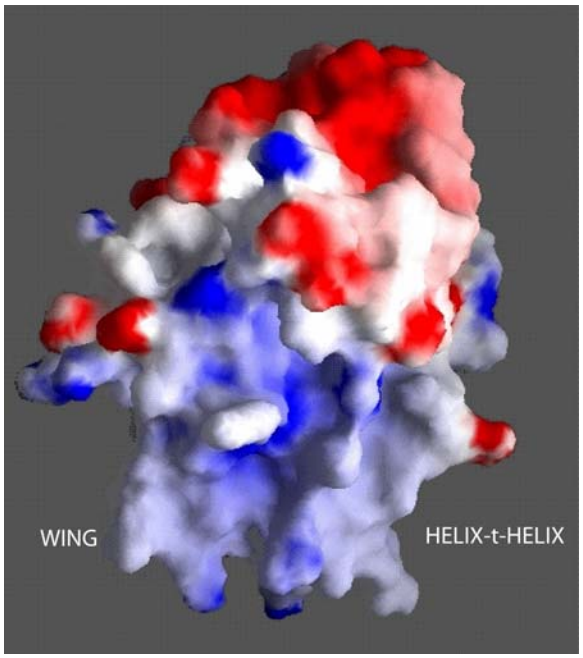
WING
HELIX-t-HELIX

(b)

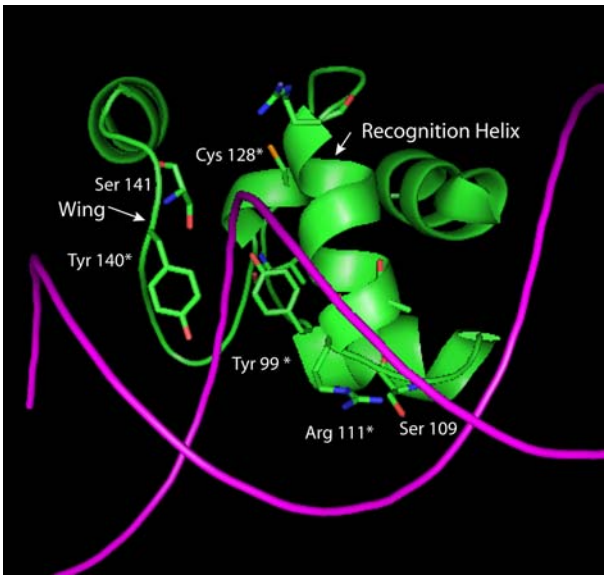
Recognition Helix
Cys 128*
Ser 141
Wing
Tyr 140*
Tyr 99 *
Arg 111*
Ser 109

(c)

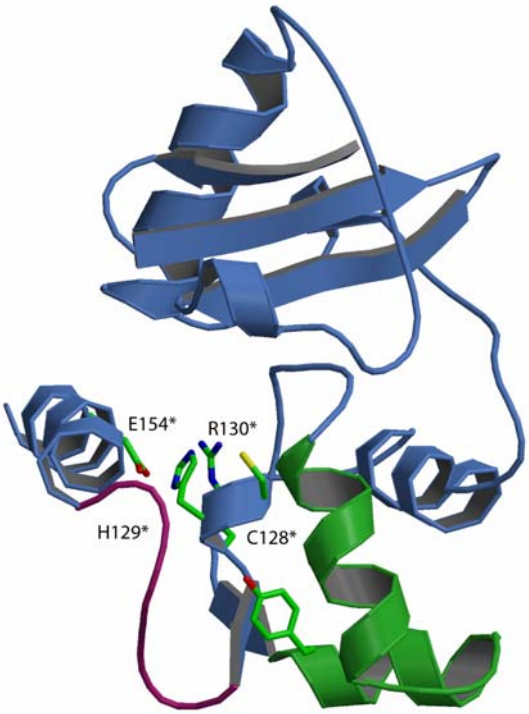
E154*
R130*
H129*
C128*